Chapter 5
Proteomic Analysis of Venomous Fang Matrix Proteins of *Protobothrops flavoviridis* (Habu) Snake

Tomohisa Ogawa, Asa Sekikawa, Hajime Sato, Koji Muramoto, Hiroki Shibata, and Shosaku Hattori

Abstract Venomous animals have specialized venom delivery apparatus such as nematocysts, stings, and fangs in addition to the poisonous organs consisting venom gland or sac, which produce and stock the venom. Snake is one of the major venomous animals, of which fangs are connected to the venom gland to inject the venom into prey. Snake's venomous fangs showed the unique characteristics including mechanical strength and chemical stability. Especially, *Protobothrops flavoviridis* (habu) snake fangs showed the resistance against its venom digestive proteases, whereas the bones and teeth of mouse were completely digested in the gastrointestinal tract, although habu fangs were also drawn into the body with the prey. These observations suggest that structural differences exist between venomous fangs and mammalian bones and teeth.

In this study, to reveal the molecular properties of venomous snake fangs, the matrix proteins of *P. flavoviridis* (habu) snake venom fang were analyzed by using proteomics experiments using 2D-PAGE and TOF MS/MS analyses. As a result, several biomineralization-related proteins such as vimentin, tectorin, adaptin, and collagen were identified in the venomous fang matrix proteins. Interestingly, the inhibitory proteins against venomous proteins such as metalloproteinase and PLA2 were also identified in fang's matrix proteins.

T. Ogawa (✉) · A. Sekikawa · H. Sato · K. Muramoto
Department of Biomolecular Sciences, Graduate School of Life Sciences, Tohoku University, Sendai, Japan
e-mail: tomohisa.ogawa.c3@tohoku.ac.jp; b1bm1012@s.tohoku.ac.jp; koji.muramoto.d5@tohoku.ac.jp

H. Shibata
Division of Genomics, Medical Institute of Bioregulation, Kyushu University, Fukuoka, Japan
e-mail: hshibata@gen.kyushu-u.ac.jp

S. Hattori
Amami Laboratory of Injurious Animals, The Institute of Medical Science, The University of Tokyo, Kagoshima, Japan
e-mail: shattori@ims.u-tokyo.ac.jp

K. Endo et al. (eds.), *Biomineralization*,
https://doi.org/10.1007/978-981-13-1002-7_5

Keywords Biomineralization · Matrix protein · Proteome · Snake · Venomous fang

5.1 Introduction

Venomous animals such as sea anemone, jellyfish, lizards, scorpion, fish, arachnids, bees, and snakes produce chemical weapon, toxic proteins, and peptides cocktail to kill and capture pray. They deliver the toxins as venom into prey through the sophisticated venom delivery systems consisting of an exocrine gland, a lumen, venom duct, and also injector such as nematocyst, sting, fangs, harpoon-like sting, and spine. These venomous apparatuses are thought to have evolved from the general biological organs, namely, an ovipositor, a tooth, radula, and dorsal fin, respectively. Snake is one of the major venomous animals, of which fangs are connected to the venom gland to inject the venom into prey. Venomous snakes can be classified into two groups according to the fang systems, front fanged (elapid and vipers) and rear fanged (grass snakes), and frontal fangs are further divided into two types, grooves and tubes (Kardong 1979; Savitzky 1980; Jackson 2002; Kuch et al. 2006). Vonk et al. (2008) reported the evolutionary origin and development of snake fangs, showing that front fangs develop from the posterior end of the upper jaw and are strikingly similar in morphogenesis to rear fangs. In the anterior part of the maxilla of front-fanged snakes, gene expression of sonic hedgehog, which is responsible among other things for the formation of the teeth, is suppressed. Despite such extensive studies and the recent genome sequence analyses for two venomous snakes, the king cobra (*Ophiophagus hannah*) (Vonk et al. 2013) and the five-pacer viper (*Deinagkistrodon acutus*) (Yin et al. 2016), the matrix proteins of venomous fangs, their evolutionary origins, and the biomineralization mechanisms of venomous fangs are still poorly understood.

Protobothrops flavoviridis (habu) snake that inhabits Ryukyu (Okinawa, Tokunoshima, and Amami) Islands are dangerous snakes having various toxic peptides and proteins (multiple protein families) as venom. Their venomous fangs are frequently lost and drawn into their own body with the prey after injection of the venom. Interestingly, venomous fangs are excreted with no change and no digestion, whereas the bones and teeth of the mouse (prey) are completely digested. These observations suggest that structural differences between venomous fangs and mammalian bones and teeth exist. In addition, it is conceivable that the adaptive evolution of the venomous organ and venomous fang bestowed them to have resistance to digestive juices. Thus, the snake fangs show the unique characteristics including mechanical strength and chemical stability.

In this study, to reveal the characteristics of habu snake fangs such as chemical stability, and their molecular evolution, proteomic analyses of fang matrix proteins were conducted by using 2D-PAGE and MALDI-TOF MS/MS.

5.2 Materials and Methods

5.2.1 Materials

The crude venomous fangs of *Protobothrops flavoviridis* (habu) snakes captured in Amami Island, Kagoshima Prefecture, Japan, were collected by dissection of the head from sacrifice. Subsequently, fangs and tissues were separately rinsed with phosphate-buffered saline and stored at −80 °C until use. Immobiline DryStrip for two-dimensional electrophoresis and the IPG buffer (pH 3–11) were obtained from GE Healthcare UK Ltd. (Buckinghamshire, England). Silver Stain MS kit was purchased from Wako Pure Chemical Industry, Ltd. (Osaka, Japan). *Achromobacter* protease I and *Staphylococcus aureus* V8 protease were obtained from Wako Pure Chemicals (Osaka, Japan) and Sigma-Aldrich Co. (St. Louis, MO, USA), respectively. ZipTip C18 was purchased from Millipore (Massachusetts, USA). All other reagents were of the best commercially available grade from Wako Pure Chemicals (Osaka, Japan) or Nacalai Tesque (Kyoto, Japan).

5.2.2 Isolation and Characterization of the Matrix Proteins from the Venomous Fang

Venomous fangs of habu snakes were decalcified with 50% formic acid at room temperature for 2 days. Then, the decalcified matrix proteins were dissolved in 6 M guanidinium hydrochloride in 50 mM Tris-HCl buffer (pH 8.8) containing 200 mM NaCl at 60 °C. After TCA-acetone precipitation, the pellet was dissolved in 8 M urea in 100 mM Tris-HCl buffer (pH 8.2) at 60 °C. For two-dimensional polyacrylamide gel electrophoresis (2D-PAGE), fang matrix proteins were directly dissolved in 400 μl of rehydration buffer (8 M urea, 4% CHAPS, 2% immobilized pH gradient (IPG) buffer (pH 3-11NL), DeStreak reagent (15 mg/ml), and 0.002% bromophenol blue) and were loaded onto IPG strips. After rehydration for 12 h, isoelectric focusing (IEF) was performed at 20 °C using the running conditions of the following focusing program: 500 V for 1 h, a gradient to 1000 V for 1 h, a gradient to 8000 V for 3 h, and 8000 V for 1.5 h (3225 V, 50 μA, 19,742 Vhs). After running IEF, IPG strips were equilibrated in a reducing equilibration buffer for 15 min and subsequently alkylated with iodoacetamide. Then, IPG strips were transferred onto 15% polyacrylamide gel (18 × 16 cm) and embedded with 0.5% agarose and electrophoresed. Gels were stained using Silver Stain MS kit or Coomassie Brilliant Blue.

5.2.3 *Proteome Analysis*

The spots on 2D gel were cut into pieces and washed with Milli-Q water. After the gels were dehydrated by acetonitrile with gentle agitation and completely dried in vacuo, gel samples were reduced by 10 mM DTT for 1 h at 56 °C. After cooling and washing by 25 mM ammonium bicarbonate buffer for 10 min, the gel samples were treated with 55 mM iodoacetamide in 25 mM ammonium bicarbonate solution in the dark. After removal of the solvent to be completely dried, gel particles were digested by *Achromobacter* protease I (Lys-C) or V8 protease at 37 °C for one night. After concentrating the digest in speed vacuum, samples were desalted on ZipTip C18 (Millipore). Samples were separated by using a DiNa Nano LC system equipped with a DiNa MALDI spotting device (KYA Technologies Co., Tokyo, Japan) and applied to MALDI-TOF MS and tandem MS/MS analysis using TOF/TOF™ 5800 Analyzer (AB SCIEX). Enzyme-digested matrix proteins without 2D-PAGE were also analyzed by nanoLC-MALDI-TOF MS/MS. Molecular masses were calibrated using the Sequazyme Peptide Mass Standards Kit (Applied Biosystems). Protein identification was performed by searching of each MS/MS spectrum against the protein sequence databases derived from the RNA-seq data of *P. flavoviridis* snake fang-forming tissues by using ProteinPilot software (version 3.0; AB Sciex) with the Paragon method.

5.3 Results and Discussion

5.3.1 *Isolation and Characterization of the Matrix Proteins from* P. flavoviridis *Venomous Fangs*

First, the decalcification conditions of venomous fangs were investigated by using hydrochloric acid and formic acid, respectively. The complete decalcification of the venomous fang without protein degradation was achieved by 50% formic acid at 30 °C for 2 days, resulting typical yield of 5.6 mg from 1.0 g of *P. flavoviridis* fangs, while the decalcification of fang by 10% HCl treatment caused the degradation of proteins (Fig. 5.1a). Then, the matrix proteins were subjected to the proteome analysis, *in-gel* enzymatic digestions for mass spectrometry characterization with 2D-PAGE and the shotgun proteomics of enzymatic digestions of total matrix proteins by nanoLC-MS/MS, respectively, after dissolved in 6 M guanidinium at 60 °C and concentrated by TCA-acetone precipitation.

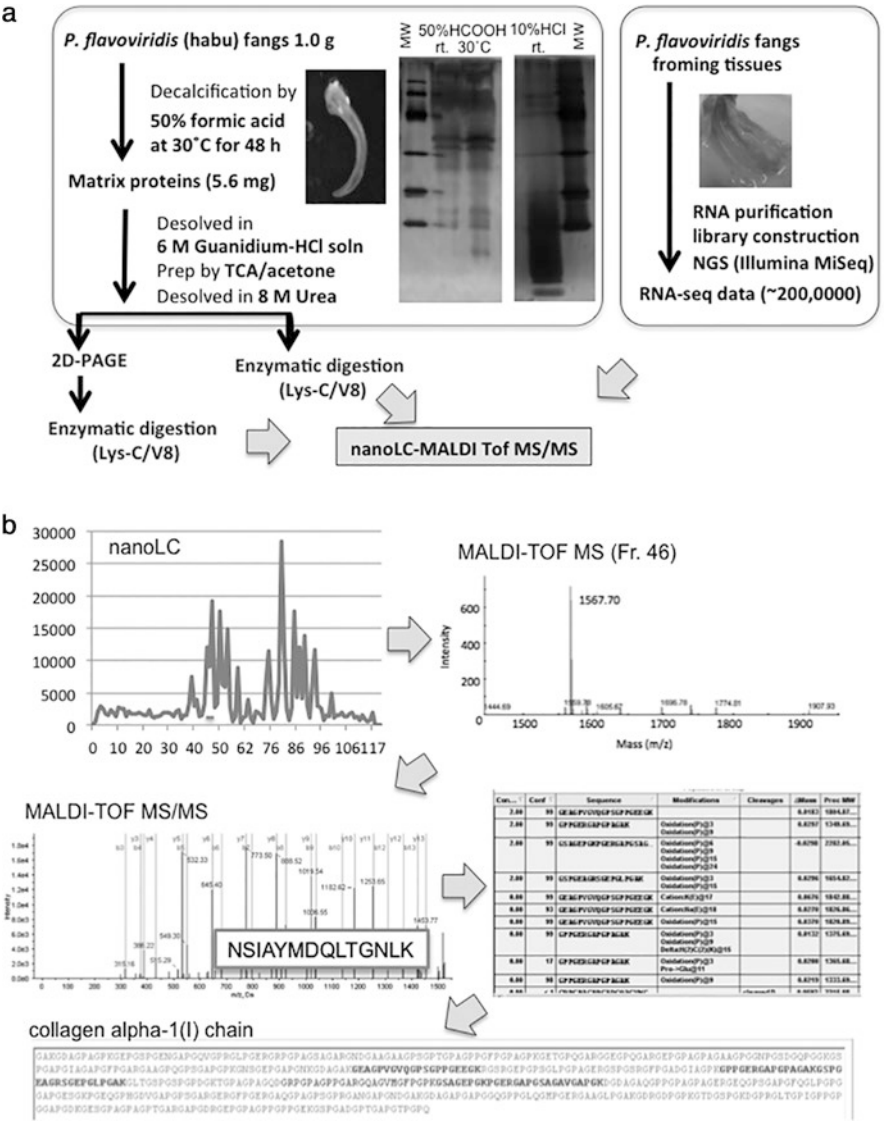

Fig. 5.1 Proteomic analysis of *P. flavoviridis* fang matrix proteins
Brief explanation of procedure through decalcification and mass spectrometry analysis (**a**) and typical profiles of digested matrix proteins on nanoLC-MALDI-TOF MS/MS (**b**)

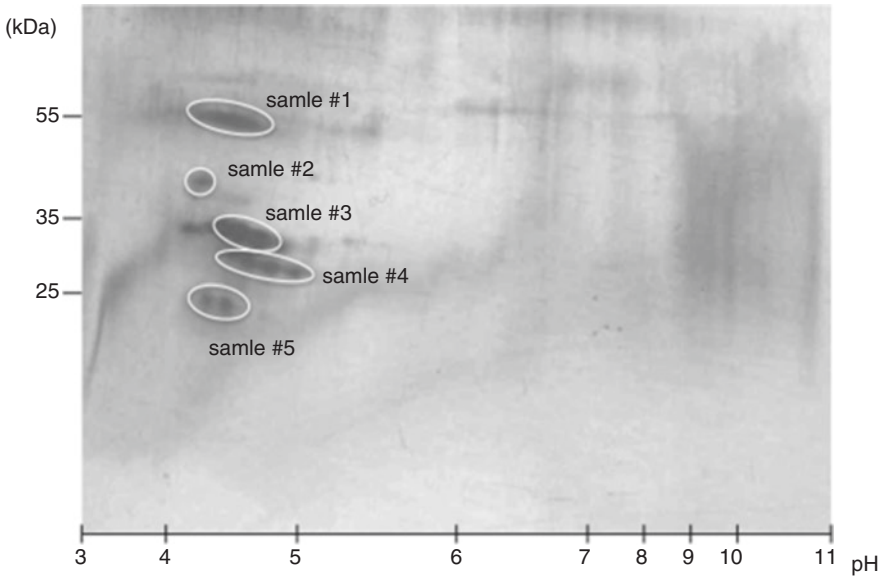

Fig. 5.2 2D-PAGE profile of *P. flavoviridis* venomous fang matrix proteins
Samples #1 to #5 were analyzed by nanoLC-MALDI-TOF MS/MS analysis after *in-gel* digestion, respectively

5.3.2 Proteome Analysis of the Fang Matrix Proteins

To identify the array of proteins in *P. flavoviridis* venomous fangs, the extracted matrix proteins were subjected to the 2D-PAGE (pH 3–11), resulting in identification in acidic region of around 20 appreciable major spots, of which pI values ranging from 4 to 6 (Fig. 5.2). These fang matrix proteins were roughly divided into five groups based on the molecular mass numbers: 55 kDa (sample #1), 40 kDa (#2), 35 kDa (#3), 30 kDa (#4), and 25 kDa (#5) proteins. Preliminary proteomic analyses of these protein spots allowed the identification of major components of fang matrix proteins including type I collagens alpha-1 and alpha-2 and UV excision repair protein RAD23-like protein (Table 5.1). Interestingly, antihemorrhagic factor HSF, which is a proteinaceous serum inhibitor against own venom metalloproteinases, was also detected as a matrix protein. However, these proteomic data from 2D-PAGE could not provide satisfactory results.

To improve the proteomic data of *P. flavoviridis* fang matrix proteins, a direct shotgun proteomic analysis was conducted. As a result of 4 independent experiments of shotgun proteomics, 36 proteins were identified as fang matrix proteins (Table 5.2). In addition to the type I collagen alpha1 (isoform X1 and X2) and alpha2 chains, the collagens type VI alpha2 and alpha3 chains and type XI alpha1 and alpha2 chains were identified. Because type I collagen has been reported to be related to the formation of dentin and enamel, contributing to the nanoscale architecture in the teeth (Wallace et al. 2010), type I collagen seems to be an important

Table 5.1 Proteomic data for 2D-PAGE analysis of *P. flavoviridis* fang matrix proteins

Sample[a]	Total	%Cov	Accession	Representative RNA-seq data	Peptides (95%)	Identified proteins
#2–1	2	7.390999794	m.3684	g.3684 ORF comp179282_c0_seq1:3–695(+)	1	Antihemorrhagic factor HSF
#3–1	4	7.451999933	m.304793	g.304793 ORF comp195637_c1_seq80:3108–4358(+)	2	Collagen alpha-1(I) chain isoform X1
#3–2	2	7.390999794	m.3684	g.3684 ORF comp179282_c0_seq1:3–695(+)	1	Antihemorrhagic factor HSF
#3–3	1.3	12.8700003	m.32414	g.32414 ORF comp189831_c0_seq6:1773–2078(+)	1	UV excision repair protein RAD23-like B
	2	12.8700003	m.32414	g.32414 ORF comp189831_c0_seq6:1773–2078(+)	1	
#4–1	2	12.30999976	m.228287	g.228287 ORF comp194729_c4_seq50:4684–5076(+)	1	Collagen alpha-2(I) chain isoform X1

[a]Sample numbers #2 to #4 correspond to the number of 2D-PAGE spots in Fig. 5.2

Table 5.2 *Protobothrops flavoviridis* fang matrix proteins identified by shotgun proteomic analyses

Trial/protein numbers	Total	% Cov	Accession	Representative RNA-seq data	Peptides (95%)	Identified proteins	Similarity (%) with mice homologs
1_1	8	9.855999798	m.304793	g.304793 ORF comp195637_c1_seq80:3108–4358(+)	4	Collagen alpha-1(I)	85
1_2	6	12.72999942	m.59430	g.59430 ORF comp191065_c4_seq27:514–1506(−)	3	Decorin	72
1_3	6	18.23000014	m.228281	g.228281 ORF comp194729_c4_seq49:3624–4235(+)	3	Collagen alpha-2(I)	75
1_4	4	3.852000087	m.380886	g.380886 ORF comp196768_c0_seq1:1–1872(+)	2	Serum albumin	32
1_5	4	10.79000011	m.280478	g.280478 ORF comp195368_c6_seq17:648–1679(−)	2	Osteonectin (SPARC)	83
1_6	2	4.098000005	m.229771	g.229771 ORF comp194758_c6_seq15:710–6349(+)	1	Collagen alpha-1(XI)	83
1_7	2	16.52999967	m.3685	g.3685 ORF comp179282_c1_seq1:1–366(+)	1	Antihemorrhagic factor HSF-like	–

1_8	2	3.260999918	m.380873	g.380873 ORF comp196660_c0_seq1:518–1624(+)	1	Biglycan	83
1_9	2	6.086999923	m.3684	g.3684 ORF comp179282_c0_seq1:3–695(+)	1	Antihemorrhagic factor HSF	–
1_10	1.7	12.8700003	m.32414	g.32414 ORF comp189831_c0_seq6:1773–2078(+)	1	UV excision repair protein RAD23-like B	73
1_11	0.4	8.122000098	m.15495	g.15495 ORF comp188251_c4_seq2:1–594(+)	0	Dual specificity protein phosphatase 3	79
1_12	0.17	2.26099994	m.302599	g.302599 ORF comp195617_c0_seq11:1965–3692(+)	0	Protein capicua homolog	66
1_13	0.14	8.653999865	m.361713	g.361713 ORF comp196120_c6_seq13:2390–3328(+)	0	L1-encoded reverse transcriptase-like protein	–
1_14	0.09	5.152000114	m.137751	g.137751 ORF comp193200_c4_seq25:1707–2699(+)	0	SLIT and NTRK-like protein 6/phospholipase A2 inhibitor-like	29
1_15	0.08	5.05400002	m.190269	g.190269 ORF comp194186_c4_seq5:195–1028(−)	0	Insulin-like growth factor binding protein 4	72
2_1	4	7.451999933	m.304793	g.304793 ORF comp195637_c1_seq80:3108–4358(+)	2	Collagen alpha-1(I)	85

(continued)

Table 5.2 (continued)

Trial/protein numbers	Total	% Cov	Accession	Representative RNA-seq data	Peptides (95%)	Identified proteins	Similarity (%) with mice homologs
2_2	2	7.390999794	m.3684	g.3684 ORF comp179282_c0_seq1:3–695(+)	1	Antihemorrhagic factor HSF	–
2_3	2	12.30999976	m.228287	g.228287 ORF comp194729_c4_seq50:4684–5076(+)	1	Collagen alpha-2(I)	75
2_4	1.4	8.147999644	m.4964	g.4964 ORF comp182948_c0_seq1:414–821(+)	1	Uncharacterized protein/SOGA3-like	–
2_5	0.8	12.8700003	m.32414	g.32414 ORF comp189831_c0_seq6:1773–2078(+)	0	UV excision repair protein RAD23-like B	73
2_6	0.05	14.00000006	m.13350	g.13350 ORF comp187844_c0_seq6:399–701(+)	0	EF-hand domain-containing family member B	58
3_1	6	20.2000007	m.228281	g.228281 ORF comp194729_c4_seq49:3624–4235(+)	3	Collagen alpha-2(I)	75
3_2	4.11	14.35000002	m.3684	g.3684 ORF comp179282_c0_seq1:3–695(+)	2	Antihemorrhagic factor HSF	–
3_3	4	3.60600017	m.304793	g.304793 ORF comp195637_c1_seq80:3108–4358(+)	2	Collagen alpha-1(I)	85

3_4	2	7.97900036	m.59432	g.59432 ORF comp191065_c4_seq31:514–1080(−)	1	Decorin	72
3_5	2	2.408000082	m.380886	g.380886 ORF comp196768_c0_seq1:1–1872(+)	1	Serum albumin	32
3_6	2	12.3999998	m.3685	g.3685 ORF comp179282_c1_seq1:1–366(+)	1	Antihemorrhagic factor HSF-like	–
3_7	2	0.585399987	m.229771	g.229771 ORF comp194758_c6_seq15:710–6349(+)	1	Collagen alpha-1(XI)	83
3_8	0.8	3.78200002	m.2124	g.2124 ORF comp168486_c1_seq1:1–717(+)	0	Peroxisome proliferator-activated receptor gamma	92
3_9	0.37	0.608900003	m.103143	g.103143 ORF comp192389_c5_seq5:3–4439(+)	0	Receptor-type tyrosine-protein phosphatase zeta isoform X2	70
3_10	0.15	1.006999984	m.314611	g.314611 ORF comp195716_c7_seq95:1655–4339(−)	0	Probable methyltransferase TARBP1	60
3_11	0.13	1.692000031	m.177447	g.177447 ORF comp193931_c1_seq1:2163–10,676(−)	0	Adenomatous polyposis coli protein	80
3_12	0.09	1.070000045	m.56612	g.56612 ORF comp190997_c1_seq12:458–4387(+)	0	BAH and coiled-coil domain-containing protein 1	60

(continued)

Table 5.2 (continued)

Trial/protein numbers	Total	% Cov	Accession	Representative RNA-seq data	Peptides (95%)	Identified proteins	Similarity (%) with mice homologs
3_13	0.09	2.153999917	m.41112	g.41112 ORF comp190336_c0_seq6:152–2104(−)	0	Leucine-rich repeat and fibronectin type III domain-containing protein 1	55
3_14	0.09	13.72999996	m.334963	g.334963 ORF comp195890_c6_seq76:1–309(+)	0	Unknown	–
3_15	0.07	7.086999714	m.14110	g.14110 ORF comp187994_c1_seq2:329–712(+)	0	39S ribosomal protein L55	43
4_1	10	11.0799998	m.380886	g.380886 ORF comp196768_c0_seq1:1–1872(+)	5	Serum albumin	32
4_2	10	25.65000057	m.3684	g.3684 ORF comp179282_c0_seq1:3–695(+)	5	Antihemorrhagic factor HSF	–
4_3	8	18.35999936	m.120416	g.120416 ORF comp192831_c6_seq13:1–1683(−)	9	Collagen alpha-1(I)X2	85
4_4	6	15.76000005	m.380873	g.380873 ORF comp196660_c0_seq1:518–1624(+)	3	Biglycan	83
4_5	6	11.77999973	m.304793	g.304793 ORF comp195637_c1_seq80:3108–4358(+)	5	Collagen alpha-1(I)X1	85

4_6	6	13.96999955	m.228235	g.228235 ORF comp194729_c4_seq37:1874–3379(+)	3	Collagen alpha-2(I)	75
4_7	4	13.84000033	m.68810	g.68810 ORF comp191390_c3_seq4:350–1024(+)	2	Transferrin-like	26
4_8	4	9.329000115	m.280478	g.280478 ORF comp195368_c6_seq17:648–1679(−)	2	Osteonectin (SPARC)	83
4_9	2	7.213000208	m.237824	g.237824 ORF comp194854_c3_seq3:504–3542(+)	1	Collagen alpha-2(VI)	55
4_10	2	2.072999999	m.85240	g.85240 ORF comp191877_c1_seq9:1401–8060(+)	1	Collagen alpha-3(VI)	55
4_11	2	1.752999984	m.164214	g.164214 ORF comp193681_c1_seq3:3–4967(+)	1	Venom factor	–
4_12	2	5.085000023	m.135289	g.135289 ORF comp193175_c0_seq8:3–1949(−)	1	Dentin matrix acidic phosphoprotein 1-like	36
4_13	2	7.97900036	m.59432	g.59432 ORF comp191065_c4_seq31:514–1080(−)	1	Decorin	72
4_14	2	12.8700003	m.32414	g.32414 ORF comp189831_c0_seq6:1773–2078(+)	1	UV excision repair protein RAD23-like B	73

(continued)

Table 5.2 (continued)

Trial/protein numbers	Total	% Cov	Accession	Representative RNA-seq data	Peptides (95%)	Identified proteins	Similarity (%) with mice homologs
4_15	2	6.25	m.209089	g.209089 ORF comp194475_c7_seq8:944–1474(+)	1	Galectin-9-like	61
4_16	1.7	13.0400002	m.1291	g.1291 ORF comp137400_c0_seq1:563–979(−)	1	Unconventional myosin-Ie	–
4_17	1.52	13.24999928	m.148536	g.148536 ORF comp193401_c3_seq19:317–1474(+)	1	Actin, cytoplasmic 1	99
4_18	0.64	2.26099994	m.302599	g.302599 ORF comp195617_c0_seq11:1965–3692(+)	0	Protein capicua homolog	66
4_19	0.47	0.630899984	m.259829	g.259829 ORF comp195117_c3_seq24:1–5709(+)	0	Collagen alpha-2(XI)	66
4_20	0.06	2.785000019	m.198369	g.198369 ORF comp194299_c9_seq1:2–2371(−)	0	Titin-like	31

component of venomous snake fang. Furthermore, the type VI collagen, which forms microfibrils and is primarily associated with the extracellular matrix of skeletal muscle and bone marrow, and type XI collagen, which is found in the cartilage of the nose and external ears in human, were also identified as matrix proteins in venomous fang, suggesting the unique distribution of type VI and type XI collagens as part of the fang matrix. On the other hand, noncollagenous dentin matrix proteins including proteoglycans (PGs), glycoproteins, serum proteins, enzymes, and growth factors are deemed to play structural, metabolic, and functional roles as key components in the mineralization process of dentin (Orsini et al. 2009). Shotgun proteomic analysis showed the fang noncollagenous dentin matrix proteins include proteoglycan such as decorin (1_2, 3_4, 4_13 in Table 5.2) and biglycan (1_8, 4_4), glycoproteins such as osteonectin (secreted protein acidic and rich in cysteine: SPARC) (1_5, 4_8), the SIBLING proteins such as dentin matrix acidic phosphoprotein 1 (4_12), and serum proteins such as albumin (1_4, 3_5, 4_1), phospholipase A_2 inhibitor (1_14) and antihemorrhagic factors, HSF (1_9, 2_2, 3_2, 4_2), and HSF-like protein (1_7, 3_6). The coexistence of these serum inhibitors as fang matrix proteins explains why venomous fang is stable against own venom enzymes compared with mouse-derived teeth and bones. Compared with the homologous proteins in mouse, several fang matrix proteins such as dentin matrix acidic phosphoprotein 1 (36%), titin-like protein (31%), transferrin-like protein (26%), and serum inhibitors including albumin (32%) and PLA2 inhibitor (29%) showed lower sequence similarities, suggesting that these differences in matrix proteins might be related to the functional differences and distinctive properties between venomous fang and mouse's teeth.

In this study, we identified 36 matrix proteins from *P. flavoviridis* snake fangs by proteomics analyses. They include proteinaceous inhibitor against own venom enzymes in addition to several types of collagens (types I, VI, and XI) and noncollagenous dentin matrix proteins. More recently, we have decoded the whole genome sequence of *P. flavoviridis* snakes (Shibata et al. 2018, in press). Further investigations are needed to elucidate the biomineralization mechanisms of venomous fang and their biological functions.

Acknowledgments The authors thank Prof. Noriyuki Satoh, Drs. Shinichi Yamasaki and Kanako Hisata, Okinawa Institute of Science and Technology Graduate University (OIST), Onna, Okinawa, for providing RNA-seq data from *P. flavoviridis* fang-forming tissues.

This study was partly supported by Grants-in-Aid of MEXT, Japan (#24651130 and #23107505 to TO). This study was also partly performed in the collaborative Research Project Program of the Medical Institute of Bioregulation, Kyushu University.

References

Jackson K (2002) How tubular venom-conducting fangs are formed. J Morphol 252:291–297

Kardong KV (1979) Protovipers and the evolution of snake fangs. Evolution 33:433–443

Kuch U, Müller J, Mödden C, Mebs D (2006) Snake fangs from the Lower Miocene of Germany: evolutionary stability of perfect weapons. Naturwissenschaften 93:84–87

Orsini G et al (2009) A review of the nature, role, and function of dentin non-collagenous proteins. Part 1: Proteoglycans Glycoproteins 21:1–18

Savitzky AH (1980) The role of venom delivery strategies in snake evolution. Evolution 34:1194–1204

Shibata H., Chijiwa T., Oda-Ueda N., Nakamura H., Yamaguchi K., Hattori S., Matsubara K., Matsuda Y., Yamashita A., Isomoto A., Mori K., Tashiro K., Kuhara S., Yamasaki S., Fujie M., Goto H., Koyanagi R., Takeuchi T., Fukumaki Y., Ohno M., Shoguchi E., Hisata K., Satoh N., and Ogawa T (2018) The habu genome reveals accelerated evolution of venom protein genes. Sci Rep (in press). https://doi.org/10.1038/s41598-018-28749-4

Vonk FJ, Admiraal JF, Jackson K, Reshef R, de Bakker MA, Vanderschoot K, van den Berge I, van Atten M, Burgerhout E, Beck A (2008) Evolutionary origin and development of snake fangs. Nature 454:630–633

Vonk FJ et al (2013) The king cobra genome reveals dynamic gene evolution and adaptation in the snake venom system. Proc Natl Acad Sci U S A 110:20651–20656

Wallace JM et al (2010) Type I collagen exists as a distribution of nanoscale morphologies in teeth, bones, and tendons. Langmuir 26:7349–7354

Yin W et al (2016) Evolutionary trajectories of snake genes and genomes revealed by comparative analyses of five-pacer viper. Nat Commun 7:13107. https://doi.org/10.1038/ncomms13107